DYNAMICS AND STATISTICS OF SIMPLE MODELS WITH INFINITE-RANGE ATTRACTIVE INTERACTION

MICKAËL ANTONI

Thermodynamique et modélisation des milieux hors d'équilibre, Laboratoire de Chimie des Systèmes Complexes, Université d'Aix-Marseille III, Av. Escadrille Normandie-Niemen, F-13397 Marseille, France
E-mail: m.antoni@lom.u-3mrs.fr

STEFANO RUFFO

Dipartimento di Energetica "S. Stecco", Universitá di Firenze, via S. Marta 3, I-50139 Firenze, Italy
INFM, Unità di Firenze, I-50125 Firenze, Italy
INFN, Sezione di Firenze, I-50125 Firenze, Italy
E-mail: ruffo@avanzi.de.unifi.it

ALESSANDRO TORCINI

Istituto Nazionale di Fisica della Materia, Unità di Firenze, Largo E. Fermi 2, I-50125 Firenze, Italy
E-mail: torcini@ino.it
URL: http://torcini.de.unifi.it/~torcini

The treatment of long-range interacting systems (including Newtonian self-gravitating systems) remains a challenging issue in statistical mechanics. Due to the lack of extensivity, they present non-standard effects like negative specific heats, which shows the inequivalence of statistical ensembles (namely, microcanonical and canonical) even in the limit of infinite number of particles ($N \to \infty$). In this paper we review a series of results obtained for one and two dimensional simple N-body dynamical models with infinite-range attractive interactions and without short distance singularities. The free energy of both models can be exactly obtained in the canonical ensemble, while information on the microcanonical ensemble and on the dynamical evolution can be derived from direct numerical simulations with simple $O(N)$ codes, which make use of mean-field variables. Both models show a phase transition from a low energy clustered phase to a high energy gaseous state, in analogy with the models introduced in the early 70's by Thirring and Hertel. The phase transition is second order for the 1D model, first order for the 2D model. Negative specific heat appears in both models near the phase transition point, but while for the 2D model it is an equilibrium phenomenon, in the 1D case it is typical of transient metastable states, whose lifetime grows with N. For both models, in the presence of a negative specific heat, a cluster of collapsed particles coexists with a halo of higher energy particles which perform long correlated flights, which lead to anomalous diffusion: the mean square displacement grows faster than linear with time. The dynamical origin of this "superdiffusion" is however different in the two models, being related to particle trapping and untrapping in the cluster in 1D, while in 2D the channelling of particles in an egg-crate effective potential is responsible of the effect. Both models are Lyapunov unstable and the maximal Lyapunov exponent λ has a peak just in the region preceeding the phase transition. Moreover, in the low energy limit λ increases proportionally to the square root of the internal energy, while in the high energy region it vanishes as $N^{-1/3}$. Since the 1D model is explicitely constructed considering the first modes of a Fourier expansion of a classical one dimensional gravity potential, the large scale properties of this model in the low-energy clustered phase resemble those of 1D gravity (mass-sheet models). The relation of both models with gravity remains to be analysed in detail by adding successive Fourier waves. However, we believe that the main dynamical effects we have found: superdiffusion and "strong" chaos (due to the evaporation and sticking of particles to the cluster) should be present also in "true" gravitational systems, and we see no obstruction that they appear also in 3D.

1 Introduction

It is well known that extensivity is an essential ingredient for building up thermodynamics from statistical mechanics questions (see e.g. Landau's textbook [1]). One is therefore naturally led to ask questions about what happens when internal energy, entropy and other thermodynamic quantities are no more extensive, i.e. when a part of a system has not the same thermodynamics properties of the whole. This problem naturally arises in Newtonian gravity, where the inherent long-range of the forces is the ultimate cause of non-extensivity, but is also present in plasma physics although the coexistence of attractive and repulsive long-range Coulomb interactions determines the screening effect which mitigates this problem. Therefore, one knows that statistical physics does not have the same strong impact for gravitational systems as it has for systems with short-range interactions and hard-cores, although one would really like to use statistical concepts in this field[a].

On the other hand mean-field models are frequently used in statistical mechanics as a first simple tool to understand the collective behavior of systems with short-range interactions and it is believed that they describe their "universal" features (such as critical exponents at phase transitions) above a certain "critical" number of neighbors. In this context, it is curious that none really posed the question of the validity of the statistical approach, considering that mean-field models (expecially those written in terms of an infinite-range Hamiltonian) explicitly violate extensivity. A reason for that lies in the fact that the thermodynamic limit is performed resorting to saddle-point techniques, which put the Hamiltonian in the explicitly decoupled form, hiding the difficulties inherent in the long-range interaction. However, all concepts related to statistical ensemble equivalence (like microcanonical/canonical equivalence) are open for such systems, and we will review in this paper models of this type for which it is indeed violated, producing effects like negative specific heats within the microcanonical ensemble, which are well known in the gravitational context [3].

The central idea contained in the papers which we are reviewing here is that it is possible to establish a close correspondence between the behaviors observed in the Hamiltonian dynamics of N-body self-gravitating systems and those of much simpler models of the mean-field infinite-range class. We have dealt only with systems in one and two spatial dimensions, but this approach can in principle be extended also to three dimensions. One of these models has been indeed rigorously derived from the self-gravitating model in one dimension, by restricting the line to a finite segment and truncating the Fourier expansion of the potential to its first wave component [4]. The two-dimensional model is less tightly related to two dimensional gravity, but arises from a similar truncation of the Fourier expansion in a box [5]. The truncation is not ineffective and introduces features which are not present in the original self-gravitating system. In one dimension, the truncated model displays a second order phase transition from a phase where the mass points are grouped in a cluster to one where they are homogeneously dispersed; this phase transition is not present in the full self-gravitating system, which

[a] Recently, Tsallis and co-workers have developed a new interesting approach based on an alternative definition of entropy, which could cope with non-extensivity[2]. The relation of their approach with our results remains to be carefully investigated

is always in the clustered phase (being the potential confining). However, we claim that many features of the clustered phase of our mean-field model are similar to those observed in the full model. Moreover, our model can be a toy system for studying phase transitions in the simple setting of one dimension (with all the computational advantages), since it is expected that phase transitions are present in three dimensions [6]. In two dimensional models some theoretical result [7] seem to suggest that a phase transition occurs at finite temperature from a clustered to a homogeneous phase.

The advantage of studying one and two-dimensional mean-field models is that their free energy in the canonical ensemble can be exactly derived by performing the mean-field limit (the infinite N limit at fixed volume), which is a reasonable surrogate of the thermodynamic limit (the infinite N limit at fixed density). Unfortunately, at variance with Thirring models [8,9], the microcanonical solution (for instance the entropy-energy relation) is not yet available for such models (although some attempts already exist along this line [10]). However, plenty of informations can be gotten from relatively fast numerical simulations, thanks to the algorithmic advantage of working with $\mathcal{O}(N)$ codes (instead of usual $\mathcal{O}(N^2)$), due to the introduction of mean-field variables. Moreover, important informations can be obtained from solving the one-dimensional non collisional Boltzmann-Poisson (BP) equation [11], although it corresponds to inverting the $N \to \infty$ limit with the infinite time limit, which can be a dangerous exchange in the presence of transient states.

In particular, from the analysis of the BP equation for the 1D model [12], it turns out that all the initial conditions with a homogeneous particle distribution and with a symmetric velocity distribution, are stable in time. Moreover, extensive dynamical simulations of the 1d and 2D model allowed us to study in detail aspects like non-ergodicity and long-time memory, that are expected phenomena in systems with non-screened long-range interactions [13].

The structure of this paper is the following. After introducing and discussing the main models in Section 2, we derive statistical equilibrium properties in Section 3. In this Section we comment also on the presence of metastable states near the phase transition point in the one-dimensional model; these states have a lifetime which grows with N. In the two-dimensional model, the microcanonical simulations reveal a region of negative specific heat. Dynamical properties are discussed in Section 4. The main effect is anomalous diffusion, superdiffusion in our case, which means that the mean square displacement of a single point mass grows in time faster than linear. In the one-dimensional model this phenomenon appears as a consequence of the presence of metastable states, i.e. it is a transient-to-equilibrium effect and is generated by the correlated trapping and untrapping of the particles in the cluster. In the two-dimensional model it is instead due to the generation of an effective mean-field potential of the egg-crate form, where particles in a certain energy range can perform long free flights; the phenomenon is destroyed by noise on the long-time span, but noise dyes out as $N \to \infty$ and thus superdiffusion extends to the time asymptotic regime. In Section 5 it is shown that the dynamics of both models is chaotic, by computing the maximal Lyapunov exponents λ. Since the systems are integrable for vanishing internal energy U and in the high energy limit, λ should exhibit a peak at intermediate energy. Indeed, λ is maximal in the phase transition region. In the high energy regime λ vanishes with an universal scaling law $\lambda = \lambda(N) \sim N^{-1/3}$, while at low energy it is positive also in the mean-field limit and increases as $\lambda = \lambda(U) \sim U^{1/2}$. In Section 6 we finally draw some conclusions and discuss some perspectives of this novel approach.

2 The Models

In this Section we introduce the 1D and 2D models. We discuss their Hamiltonians and equations of motion by introducing the mean-field variables. We also give a brief description of the phenomenology and of the tools that have been introduced for their study.

2.1 One dimensional model

This first model describes a collection of N identical particles that move under their mutual gravitational-like attraction. Each particle is a mass point and boundary conditions are periodic. Particles are therefore constrained to move on the unit circle, *i. e.* in a one dimensional geometry. The total energy is constant and given by [4]:

$$H = \sum_{i=1}^{N} \frac{p_i^2}{2m} + \frac{m^2}{2N} \sum_{i,j=1}^{N} \Big(1 - \cos(\theta_i - \theta_j)\Big) = K + V, \qquad (1)$$

where $\theta_i \in]-\pi, \pi]$ is the coordinate of the i-particle, p_i its conjugate momentum and m the mass of the particles. A time-discrete version of this model has been previously introduced by Kaneko and Konishi [14]. The system is isolated, total momentum is conserved and can be set to zero without loss of generality. K and V are the kinetic and potential energy respectively. As the latter has no singularity when $i = j$, the particles do not collide but smoothly cross through one other. This shows up clearly in the equations of motion

$$\ddot{\theta}_i = \frac{\dot{p}_i}{m} = -\frac{m}{N}\sum_{j=1}^{N}\sin(\theta_i - \theta_j) \ , \tag{2}$$

since they correspond to a system of fully coupled pendula.

The potential energy is rescaled by $1/N$ in order to get a finite specific energy $\mathcal{H} = H/N$ in the thermodynamic limit $N \to \infty$, hence the potential is thermodynamically stable ($H \geq E_0 N$). The characteristic period t_c of particle motion is then an intensive quantity, given by $t_c = 2\pi/\sqrt{m}$. In the large N limit, particles can be treated in a mean-field approximation and the distribution functions can be computed using Poisson-Boltzmann techniques [11,15]. These techniques have been used in a large variety of dynamical systems (plasmas, galaxies, fluids) where particle-particle collisions can be neglected when compared to the particle-mean-field coupling. For model (1), the mean-field variable writes:

$$\mathbf{M} = (M_x, M_y) = \frac{1}{N}\sum_{j=1}^{N}\mathbf{s}_j \quad , \quad \text{with} \quad \mathbf{s}_j = (\cos\theta_j, \sin\theta_j) \quad . \tag{3}$$

With these definitions, Eq. (2) reduces to that of a single perturbed pendulum

$$\ddot{\theta}_i = -M\sin(\theta_i - \phi) \tag{4}$$

where we have set the mass $m = 1$ for simplicity and $\phi = \arg(\mathrm{M})$ is the phase of the mean-field. Both M and ϕ are scalar quantities that depend on time through $\theta's$ and their time evolution describes the collective dynamics of the system.

The single-particle dynamics is ruled by the Hamiltonian

$$h_i = \frac{p_i^2}{2} + 1 - M_x\cos(\theta_i) - M_y\sin(\theta_i) = K_i + V_i \tag{5}$$

which is non authonomous, since it depends on the mean-field, which reflects the collective dynamics of the model. Hence, each particle moves in a mean-field potential V_i determined by the instantaneous positions of all the other particles of the system.

The thermodynamics of model (1) can be derived theoretically in the canonical ensemble (see Sect. 3). It shows a second-order phase transition at a critical value of the internal energy $U_c = H_c/N = 0.75$ between a collapsed phase, where a single cluster is present, and a homogeneous phase, where particles are uniformly distributed on the circle. The development of the cluster in the collapsed phase corresponds to the well known Jeans instability for self-gravitating systems [11].

Numerical simulations of self-gravitating systems in their collapsed phase and initially far from equilibrium, usually reveal two evolution mechanisms: i) collective phenomena that involve almost all the particles and that rapidly drive the system into a quasi-stationary configuration; ii) individual effects that rule the successive slow relaxation to equilibrium. On short time scales, spiral structures are often developed to eliminate the excess of kinetic energy [4]; they are due to the formation phase-space domains with an excess or depletion of particles. These structures are robust enough to resist individual particle effects and are known to prevent the system from reaching equilibrium [16]. They are similar to the Dupree structures observed in plasmas where they inhibit Landau damping and constitute an important element of Vlasov turbulence [17].

Model (1) contains only one spatial scale, the length 2π; this reflects in the presence of a single modulation of the particle density (the cluster). However, this model belongs to the family of N-body Hamiltonian systems that write

$$H_s = \sum_{i=1}^{N} \frac{p_i^2}{2m} + \frac{m^2}{2N} \sum_{i,j=1}^{N} \sum_{n=0}^{s} \frac{1}{k_n^2} \left(1 - \cos\Big[k_n(\theta_i - \theta_j) \Big] \right), \qquad (6)$$

where $k_n = 2n + 1$ and where the parameter s counts the number of Fourier harmonics [4,18]. The interest in this family of Hamiltonians lies on the fact that in the limit $s \to \infty$ they write

$$H_\infty = \sum_{i=1}^{N} \frac{p_i^2}{2m} + \frac{m^2}{2N} \sum_{i,j=1}^{N} |\theta_i - \theta_j| = \sum_{i=1}^{N} \frac{p_i^2}{2m} + 2\pi G \frac{m^2}{N} \sum_{i,j>i} |\theta_i - \theta_j|, \quad (7)$$

where G is the gravitational constant and the customary dimensionless units $1 = 2\pi G$ have been chosen [19]. Up to the $1/N$ scaling constant of the potential, this Hamiltonian is the one of a collection of N identical planar mass sheets of constant mass surface density μ evolving in one dimension perpendicular to their surface. This model was originally introduced to describe the dynamics of stars evolving in the neighborhood of a flattened galaxy [20]. For the Poisson-Boltmann limit to exist, one must require the the total mass $\mu N = m$ remains finite when one lets $N \to \infty$. Then

$$\mathcal{H}_\infty = \frac{H_\infty}{N} = \sum_{i=1}^{N} \frac{\bar{p}_i^2}{2\mu} + 2\pi G \mu^2 \sum_{i,j>i} |\theta_i - \theta_j|, \qquad (8)$$

where $\bar{p}_i = p_i/N$ are the scaled momenta. We would like to notice that the Hamiltonian H_∞ can be transformed in that corresponding to the usual gravitational 1D model also by simply multipling the time units by a factor $\sqrt{N}$, this obviously corresponds also to rescale the energy units by a factor N [21].

The dynamics of the mass sheet model involves an interplay of all the spatial scales, which is the source of its metastability. The advantage of using models (6) is that they allow a selection of a limited number of modes, through the tuning of the parameter s; the qualitative changes in the dynamical and in the thermodynamical behavior can be followed by adding higher Fourier components. Such a multiscale approach is based on the mean-fields $\mathbf{M}_{k_n} = 1/N \sum_j \mathbf{s}_{j,k_n}$ with $\mathbf{s}_{j,k_n} = (\cos k_n\theta_j, \sin k_n\theta_j)$. This approach to self-gravitating systems is similar to the one proposed in Ref. [22] where a weak formulation based on a smoothed-out gravitational potential is introduced. We expect that the large scale properties won't be strongly modified by the introduction of smaller spatial scales. However, the balance between collective (large scale) and individual (small scale) effects might depend crucially on the number of Fourier components. The investigation of the properties of model (1) is thus the very first step in the investigation of Hamiltonian (8). Indeed, one major difference is that while model (1) has a second-order phase transitions, model (8) has no phase transition. The absence of phase transitions is a trivial consequence of the existence of the scale transformation $\theta_i \to \alpha^2\theta_i$, $p_i \to \alpha p_i$, $t \to t/\alpha$, which transforms the energy as $\mathcal{H}_\infty \to \alpha^2\mathcal{H}_\infty$ and leaves the equations of motion unchanged. Thus, if $\alpha > 1$ states corresponding to a larger energy coincide with those at a shorter time. Therefore, increasing the energy cannot produce any phase transition, but it is like observing the dynamics on a shorter time scale. Hamiltonian (8) is always in the clustered phase, since the potential is always confining. To induce a phase transition one must explicitly introduce a scale in the model (this has been recently done for the spherically concentric mass shell model in Ref. [23]). An open question is how the phase transition disappears in the $s \to \infty$ limit, and a related one is whether phase transitions are present in 2D and 3D self-gravitating systems [6].

2.2 Two dimensional model

We have also studied a two dimensional model, that can be viewed as a generalization of the one dimensional model introduced in the previous Subsection. We consider a system of N pointlike identical particles with unitary mass moving in a 2-D box with periodic boundary coditions. The dynamics is ruled by the Hamiltonian

$$
\begin{aligned}
H &= \sum_{i=1}^{N} \frac{p_{i,x}^2 + p_{i,y}^2}{2} \\
&+ \frac{1}{2N} \sum_{i,j}^{N} \left[3 - \cos(x_i - x_j) - \cos(y_i - y_j) - \cos(x_i - x_j)\cos(y_i - y_j) \right] \\
&= K + V \quad , \qquad (9)
\end{aligned}
$$

where $(x_i, y_i) \in]-\pi, \pi] \times]-\pi, \pi]$, $(x_i, p_{i,x})$ and $(y_i, p_{i,y})$ are pairs of conjugate variables. K (resp. V) is the kinetic (resp. potential) energy. The reference energy is chosen in order to ensure the vanishing of the total energy of the system when all the particles are placed in the same position ($V = 0$) at rest ($K = 0$). Without the presence of the third term in the potential the particles would move independently along the x and y-directions according to the previously introduced 1-D potential (1). The interparticle potential appearing in (9) mimicks the Fourier expansion in a periodic square box of side $L = 2\pi$ of a 2-D self-gravitating Newtonian potential ($\log |r|$, being r the interparticle Euclidean distance), restricted to its first three terms $(n_x, n_y) = (0,1), (1,0), (1,1)$, where $k_x = 2\pi n_x/L$ and $k_y = 2\pi n_y/L$ are the wave numbers along the two directions. Interactions of the $\log |r|$ type arises also for point vortices in 2D Eulerian turbulence [24], and our approach could be fruitfully extended to this case.

The equations of motion for the coordinates x_i are

$$
\ddot{x}_i = -\frac{1}{N} \sum_{j=1}^{N} \left[\sin(x_i - x_j) + \sin(x_i - x_j)\cos(y_i - y_j) \right] \qquad (10)
$$

and those for y_i are obtained exchanging $x \leftrightarrow y$, due to the symmetry of (9).

Previous investigations of model (9) [5] have revealed that at low energy $U = H/N$ the particles, due to attractive coupling, collapse into a unique cluster, with U-dependent spatial extension. This clustered phase survives up to a critical energy $U_c \sim 2.0$ (numerically determined from an implicit equation derived in the canonical ensemble), where a first-order phase transition occurs to a homogeneous phase. This transition will be discussed in more detail in the next Section. The collective behaviour is evidenced by the following mean-field variables

$$
\mathbf{M}_1 = (< \cos(x) >_N, < \sin(x) >_N) = M_1 \;\; (\cos(\phi_1), \sin(\phi_1)) \qquad (11)
$$

$$
\mathbf{M}_2 = (< \cos(y) >_N, < \sin(y) >_N) = M_2 \;\; (\cos(\phi_2), \sin(\phi_2)) \qquad (12)
$$

$$\mathbf{P}_1 = (< \cos(x+y) >_N, < \sin(x+y) >_N) = P_1 \ (\cos(\psi_1), \sin(\psi_1)) \qquad (13)$$

$$\mathbf{P}_2 = (< \cos(x-y) >_N, < \sin(x-y) >_N) = P_2 \ (\cos(\psi_2), \sin(\psi_2)) \qquad (14)$$

where $< .. >_N$ denotes the average over all the particles in the system. The moduli $M_{1,2}$ and $P_{1,2}$ are maximal and equal to 1 when all the particles have the same position and their value decrease when the spatial distribution of the particles extends. For a homogeneous distribution, according to the central limit theorem, $M_{1,2} \approx P_{1,2} \approx O(1/\sqrt{N})$. These quantities are the order parameters characterizing the degree of clustering of the system.

By reexpressing the equation of motion (10) for both coordinates x and y in terms of the mean-field variables, one straighforwardly shows that the time evolution of the $i-$th particle is ruled in a way similar to the 1D model by the following single particle non autonomous Hamiltonian :

$$\begin{aligned} h_i &= \frac{p_{x,i}^2 + p_{y,i}^2}{2} + \Big[3 - M_1 \cos(x_i - \phi_1) - M_2 \cos(y_i - \phi_2) \\ &- \frac{1}{2} P_1 \cos(x_i + y_i - \psi_1) - \frac{1}{2} P_2 \cos(x_i - y_i - \psi_2) \Big] \\ &= K_i + V_i \quad . \end{aligned} \qquad (15)$$

Since V is invariant under the transformations $x \leftrightarrow -x$, $y \leftrightarrow -y$ and $x \leftrightarrow y$, it turns out that in the mean-field limit ($N \to \infty$ with constant $U = H/N$), $M_1 = M_2 = M$ and $P_1 = P_2 = P$.

3 Equilibrium properties

In this Section we will mainly discuss the canonical equilibrium exact solutions of the previoulsy introduced 1D (1) and 2D (9) self-gravitating models and we will compare these solutions with the result of the microcanonical simulations. The canonical free energy is easily obtained in both cases by resorting to an inverse Gaussian transformation (sometimes called the Hubbard-Stratonovich trick) and evaluating an integral with saddle-point techniques. For the 1D model (1), we have shown that the phase transition between the collapsed and the homogeneous phase is a second order phase transition. For the 2D model (9) the transition is instead of first order. Microcanonical simulations reveal the presence of a negative specific heat region near the phase transition for both the 1D and the 2D model, but for the former case this is only a transient effect (however, the transient grows with the number N of point masses). Ensemble inequivalence and negative specific heats are indeed rather familiar to astrophysicts and appear in the phenomenon known as the *gravothermal* *catastrophe* [25]. These observations confirm the conjecture of Lynden-Bell [25,3] and demontrate on a simple model that the equivalence among statistical ensembles is violated due to the long-range nature of the forces and to the absence of repulsive hard-cores.

3.1 One dimensional model

The one-dimensional model of Eq. (1) can be exactly solved in the canonical ensemble. Its free energy

$$F = - \lim_{N \to \infty} \frac{1}{N} \ln \int \prod_i d\theta_i dp_i \exp(-H/T) \tag{16}$$

is given by the expression

$$-F/T = \frac{1}{2} \ln(2\pi T) - \frac{m}{2T} + \max_x \{ \frac{-x^2 T}{2m} + \ln(2\pi I_0(x)) \} \tag{17}$$

where the max is obtained by solving the consistency equation

$$\frac{I_1(x)}{I_0(x)} = \frac{Tx}{m} \ , \tag{18}$$

where I_0 and I_1 are respectively the zero and first order modified Bessel functions. In the following we will adopt the value $m = 1$, without loss of generality. Eq. (18) has the unique solution $x = 0$, corresponding to the vanishing mean-field region $M = 0$, for $T \geq 0.5$; it has instead two symmetric nonvanishing solutions, corresponding to a nonvanishing value of M for $T < 0.5$. This latter is the clustered phase and the ratio M/T determines the average size of the cluster (which becomes infinitely narrow, i.e. it collapses to a point, only in the zero temperature limit). The temperature dependence of the mean field M is exactly derivable and it is shown in the inset of Fig. 1 by the continuous line. The temperature-energy relation can be also derived using the standard formula $U(T) = \partial(F/T)/\partial(1/T)$ and is reported in the same figure. This model has therefore a second order phase transition at the critical temperature $T_c = 0.5$, corresponding to the critical energy $U_c = 3/4$. The dynamical time averages of the same quantities can be determined by computer simulations. Being the model Hamiltonian, the energy is fixed by the initial state and temperature is dynamically determined by computing the average kinetic energy per particle, and waiting for long time relaxation.

In all energy ranges, except close to the critical point, every chosen initial state relaxes quite fast to the canonical curves of M vs. U and T vs. U; finite N corrections are visible in Fig. 1. On the contrary, in a region just below the critical point (evidenciated by the vertical line in Fig. 1) initial

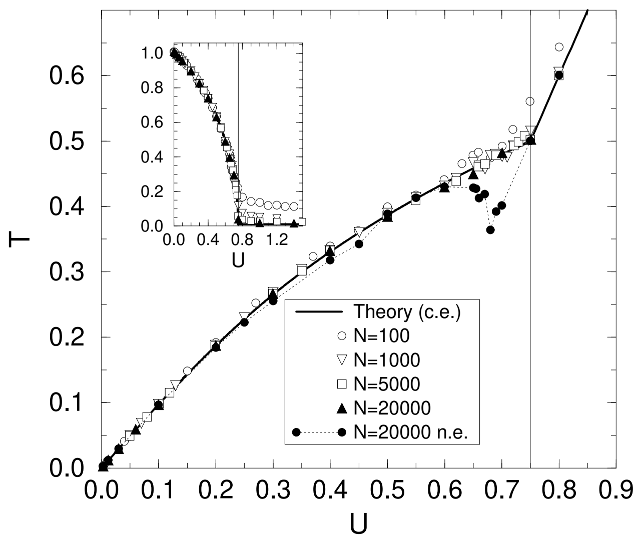

Figure 1. Temperature T versus the internal energy U for the 1D model (1). The full curve is obtained theoretically in the canonical ensemble ($N \to \infty$). The points are the result of microcanonical simulations with an increasing number of mass points, in particular the full circles refer to an initial "water bag distribution". In the inset, the mean-field variable M vs. U is reported with the same notation. The horizontal lines indicates U_c.

states of the "water-bag" class (uniformly distributed momenta in a fixed interval symmetric around zero and all positions at $\theta_i = 0$) show a relaxation to metastable non-equilibrium states, whose T vs. U curve has two main features: i) for $U > 0.67$ the points lye on the continuation for $U < 3/4$ of the line $T = 2U - 1$; the corresponding states are gas-like, with zero magnetization (uniform in space) and have non-Gaussian tails in momentum; ii) for $0.6 < U < 0.67$, T decreases when U increases, this is the negative specific heat region. All these latter points, obtained for a system of $N = 20,000$ point masses, relax very slowly to the canonical curve (as shown by the behavior of their relative Boltzmann entropy in Fig. 2a) in a time which increases linearly with the number N of particles of the system Fig. 2b. Ideally, if one would have prepared a system with an infinite number of particles, this would not have relaxed to the canonical equilibrium. The metastability of our model is not as strong as the one encountered for disordered systems (where the relaxation time diverges exponentially in N), it is of the same type as the one found for the mass-sheet model and for plasma models as reviewed in Ref. [18]. Its origin lies in the complex structure of the chaotic web through which the orbit channels in phase-space (see further comments Section 4.1).

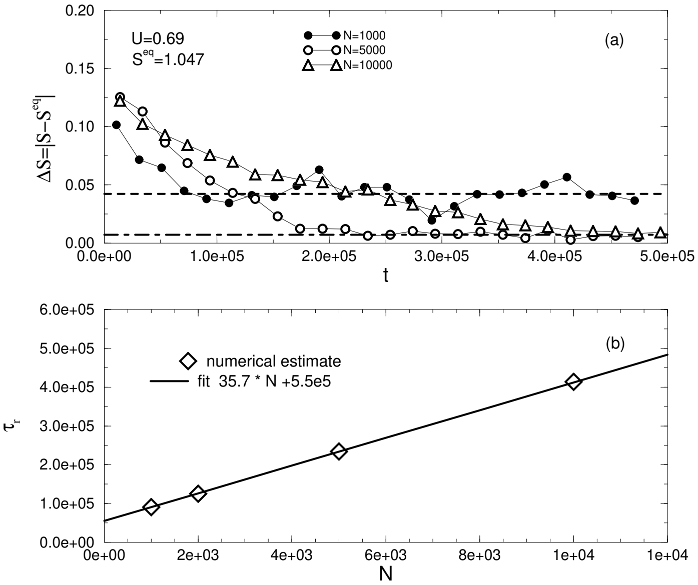

Figure 2. a) Absolute difference with respect to the equilibrium Boltzmann entropy for the momentum distribution vs. time t. Relaxation slows down for increasing N. b) A plot of the relaxation time τ_p vs. the number of particles N. The full line is a best linear fit to the data.

The equilibrium behavior discussed above and depicted in Fig. 1 can be derived also using the non-collisional Boltzmann-Poisson (BP) equation in two different ways: i) imposing the maximal entropy principle, as done in Ref. [11]; ii) looking for solutions with a Gaussian shape in momentum and a factorized stationary distribution function $f(\theta, p, t) = f_1(\theta) f_2(p)$ [15]. To our knowledge, the fact that the canonical equilibrium solution coincides with the one given by the BP equation is a novel feature, which deserves further investigations for other models. The use of the BP equation gives access also to the one-particle distribution function $f(\theta, p, t)$, on which numerical checks have been performed in Ref.[15]. A feature which remains unexplored in the context of the

PB equation is metastability, but recently one of the authors [12] has proven, using the expression of the evolution operator in terms of Lie brackets [26], that initial states symmetric in momentum $f_1(p) = f_1(-p)$ and uniform in position do not evolve in time to all orders in perturbation theory. This is a first sign of metastability in the PB context, where since one is treating directly the $N \to \infty$ limit, metastability manifests itself in a multi-stability. Finally, let us mention that recently in Ref. [27] it has been shown that the transition observed for the model (1) is associated, in the mean-field limit, to a change in the topology of the corresponding configuration space.

3.2 Two dimensional model

Model (9) can be solved in the canonical ensemble as in the 1D and all its equilibrium features can be exactly derived in the mean-field limit, using again saddle-point technique [5]. We do not reporte here the explicit expression for the free energy, that is already reported elsewhere [5]. The single particle potential V_i for the 2D case (15) is reported in Fig. 3, it has a shape similar to the so-called egg-crate potential studied in Ref. [28]. The potential is periodic along the two spatial directions and in each elementary cell has 4 maxima ($V_M = 3 + 2M - P$), 4 saddle points ($V_s = 3 + P$) and a minimum ($V_m = 3 - 2M - P$). The depth of the potential well is $(V_s - V_m)$ and the center of the cluster in the collapsed phase coincide with the position of the minimum of the potential. In the limit $U \to 0$, M and $P \to 1$ and therefore $V_M \to 4$, $V_s \to 3$ and $V_m \to 0$. In this limiting situation all the particles are trapped in the self-consistent potential well. Increasing U, the kinetic energy produces an evaporation of the particles from the cluster. This implies that also the values of M, P and of the well depth decrease (see Fig. 4). For $U \geq U_c$, there are no more clustered particles and in the limit $N \to \infty$ the single particle potential becomes flat $V_M = V_s = V_m = 3$ and time independent.

However, due to finite N effects, the instantaneous mean-field variables fluctuate with a typical time $\mathcal{O}1$ within the statistical band range $\sim 1/\sqrt{N}$. This implies that in the collapsed phase the particles move in a fluctuating potential.

In Fig.5 the temperature T is reported as a function of U. Above $U_c \sim 2.0$, T increases linearly with U indicating that the system behaves like a free particle gas. In the collapsed phase, the tendency of the system to collapse is balanced by the increase of the kinetic energy [29]. This competition leads initially (for $0 < U < 1.8$) to a steady increase of T, followed (for $1.8 < U < U_c$) by a rapid decay of T. This yields a negative specific heat as illustrated in the inset of Fig.5. These results are in full agreement with theoretical

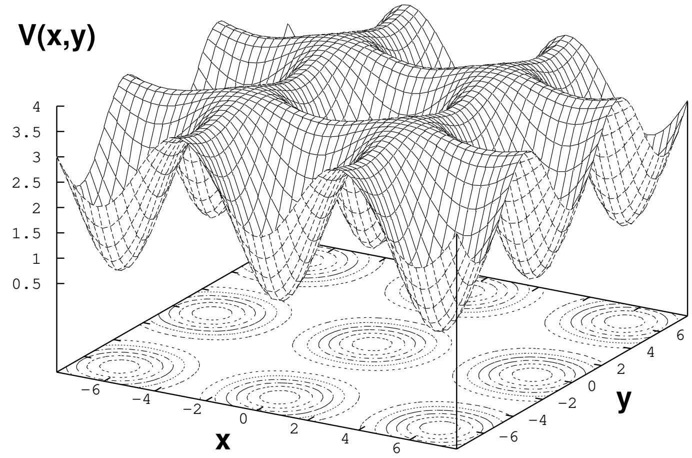

Figure 3. Instantaneous single particle potential $V(x,y)$ together with its contour-plot for $U = 1.00$ and $(x,y) \in [-5\pi/2, 5\pi/2]^2$.

predictions based on the analysis of a simple classical cell model [9] and with numerical findings [29,30] for short ranged attractive potentials without hard-cores. The phenomenon of negative specific heat can be explained within a microcanonical approach with an heuristic argument [9]: approaching the transition, a small increase of U leads to a significative reduction of the number of collapsed particles (as confirmed from the drop exhibited by M and P for $U > 1.8$ in Fig.4); as a consequence the value of V grows and, due to energy conservation, the system becomes cooler.

Our data confirm also another important prediction of Hertel and Thirring [8,9]: the non-equivalence of canonical and microcanonical ensemble nearby the transition region. In the inset of Fig. 5 we report the microcanonical findings, obtained by direct simulations, and the theoretical canonical results. These two sets of data coincide everywhere, except in the energy interval $1.6 \leq U \leq 2.0$. The discrepancy is due to the impossibility of the canonical ensemble to exhibit a negative specific heat, a prohibition that does not hold for the microcanonical ensemble. Our theoretical estimation of the Helmholtz

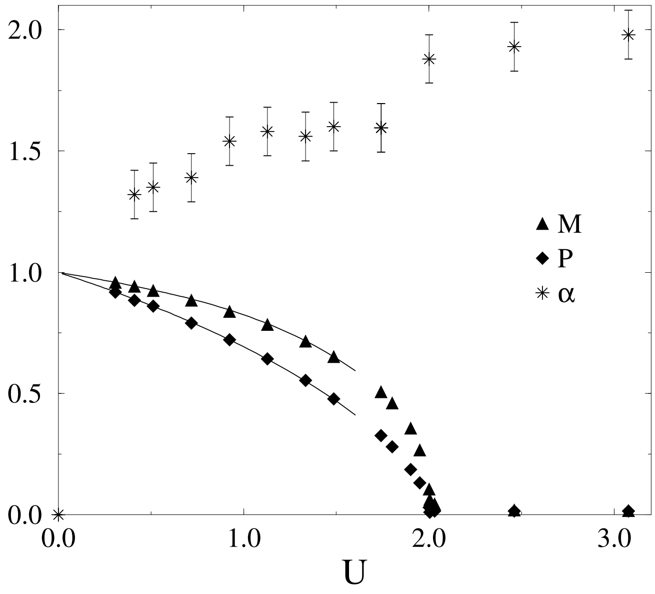

Figure 4. Meanfield quantities M and P as a function of U. The solid line refer to canonical results analytically estimated, while the symbols to microcanonical results obtained via numerical simulations. The exponent α defined in eq. (20), are also shown (asteriskes). The data have been obtained with $N = 4,000$ (apart few points with $N = 10,000$) and averaged over a total integration time of order 10^6.

free energy $F = F(T)$ reveals that usually F has an unique minimum. For $T < 0.5$ the minimum F_c corresponds to non zero values of M and P (i.e. to the collapsed phase), while for $T > 0.55$ the minimum F_H is associated to $M = P = 0$ (i.e. to the homogeneous phase). In the region $0.5 < T < 0.55$, both minima F_c and F_H coexist as local minima of the free energy. However, for $T < T_c = 0.54$ the collapsed phase is observed because $F_c < F_H$, while for $T > T_c$ the homogeneous phase prevails since $F_H < F_c$. At $T = T_c$ the two minima are equivalent and a jump in energy from $U(T_c^-) \approx 1.6$ to $U(T_c^+) \approx 2.0$ is observed. This transition is therefore first order [29], with a finite latent heat $U(T_c^+) - U(T_c^-)$.

At variance with the 1D model, there is no sign of metastability in the 2D (apart eventually at U_c), at least for what concerns the thermodynamical properties. All the data reported in Figs. 4 and 5 correspond to the time asymptotic state, also in the negative specific heat region. This is the main

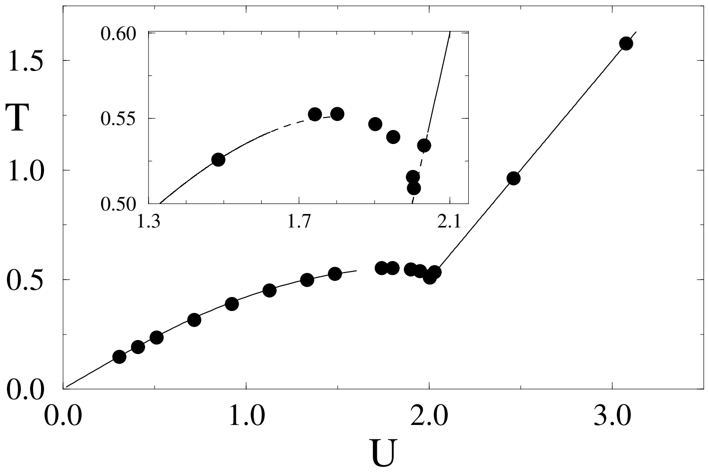

Figure 5. Temperature T as a function of the internal energy U for the 2D model. The solid line refers to analytical results obtained within the canonical ensemble, while the full circles to microcanonical simulation results. The inset is an enlargement of the transition region: the full curves (resp. dashed) refer to the absolute (resp. relative) minimum of the free energy $F(T)$.

not yet understood difference between the 1D and the 2D model.

4 Dynamical Properties

In this Section we discuss the main dynamical properties of the 1D and 2D models. The most important phenomenon is correlated to trapping and untrapping of particles within the cluster in the low energy collapsed phase. this effect produces an anomalous diffusion (superdiffusion) of particles, which has a finite time span, being destroyed by relaxation to equilibrium in the 1D model and by noisy fluctuactions (due to the finite number of particles) of the single-particle potential in the 2D model. However, for both models in the mean-field limit superdiffusion should be present at any time.

4.1 One dimensional model

The single particle Hamiltonian (5) of the 1D model is that of a perturbed pendulum. The perturbation has two different sources in the time dependence of M, which generates the stochastic layer around the separatrix, and in that of ϕ, which is the main origin of the trapping/untrapping phenomenon in the nonlinear resonance of the pendulum. In Fig. 6 we show a snapshot taken at some large time of the particles which were initially put in a "water-bag" initial condition: near the center of the resonance particles librate forming a spiral whose branches touch the separatrix region. The unperturbed separatrix is drawn making reference to the asymptotic value of M and its center in momentum is slightly displaced from zero, because the cluster is slowly drifting [4]. Out-of-resonance particles are capable of performing long flights if energy is large enough. A typical trajectory of a particle is shown in Fig. 7 and reveals the presence of tracts of almost free motion with a typical positive or negative speed, interrupted by tracts where the particle is trapped in the cluster, performing with it a much slower motion. It has been shown in Ref. [31] that the motion is "superdiffusive", i.e. the mean square displacement $< \theta^2 >$ (where the average is taken over the particles and over distinct time origins) has the anomalous scaling

$$< \theta^2 > \sim t^\alpha \tag{19}$$

with $\alpha = 1.4 \pm 0.1$ in a given energy range just below the phase transition point, $0.6 < U < 0.7$, and for a finite time. When the system relaxes to thermal equilibrium, diffusion becomes normal ($\alpha = 1$), but the time taken to do this change increases with N, exactly as the relaxation time to equilibrium. We can then state that in the thermodynamic limit the motion is superdiffusive forever, when starting from a non-equilibrium (e.g. "water-bag") initial state. It is suggestive, and deserves further investigation, the fact that superdiffusive motion is found in the region of negative specific heat, where a core of collapsed trapped particles coexists with a "halo" of almost free particles.

4.2 Two dimensional model

We concentrate in this Subsection on the description of the transport properties of the 2D model (9). In the collapsed phase each particle of our system moves in the single particle potential $V_i = V_i(t)$ (see Fig. 3) of the egg-crate form [28]. For a single particle moving in such fixed potential the self dynamics is known to be anomalously diffusive when the particle is channeling, *i.e.* when its energy lies between V_M and V_s [28]. This anomalous behaviour is due to the competition of laminar and localized phases. Indeed, channeling particles intermittently show an almost ballistic motion along the channels of the potential interrupted by localized sequences, where the particles bounces back and forth on the maxima of the potential.

Usually anomalous diffusion has been studied in systems with a few de-

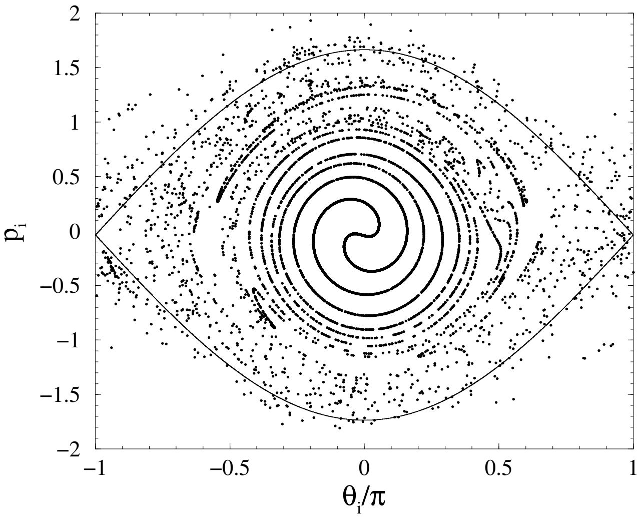

Figure 6. Snapshot at some large time of the single-particle phase-space for an initial "water bag" distribution at $U = 0.4$ and with $N = 10,000$ for the 1D model. The full line indicates the separatrix of the unperturbed pendulum drawn at the corresponding equilibrium value of M.

grees of freedom [32,28]. Only few attemps have been made to consider N-body dynamics with $N \gg 1$ [14,33,34].

In this Subsection we give some indications relative to the basic dynamical mechanisms governing single particle transport. To this aim, we consider the time dependence of the mean square displacement (MSQD), that usually reads as

$$< r^2(t) > \propto t^\alpha \tag{20}$$

where the average $< . >$ is performed over different time origins and over all the particles of the system. The transport is said to be anomalous when $\alpha \neq 1$: namely, it is subdiffuse if $0 < \alpha < 1$, superdiffusive if $1 < \alpha < 2$ and ballistic for $\alpha = 2$ [28,35,32]. The usual Einstein diffusion law corresponds to $\alpha = 1$ and in 2D can be written as $< r^2(t) >= 4Dt$, where D is the self-diffusion coefficient.

If one considers a single particle with an initial energy between V_M and V_s and follows its trajectory for some time it displays features quite similar to the so-called Lévy walks [32] (see Fig.8). This kind of trajectories are usually identified when anomalous diffusion occurs.

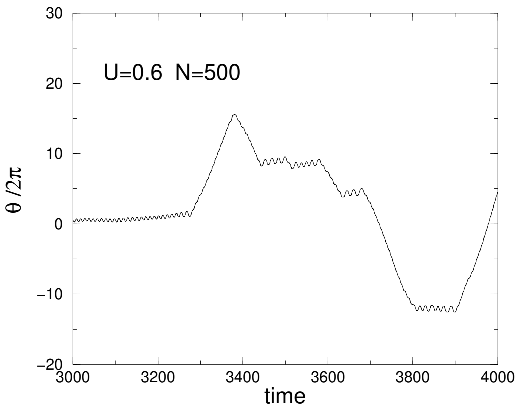

Figure 7. Free flights and trapped motions of a particle in the 1D model for $U = 0.6$, $N = 500$ and a "water bag" initial condition.

As we already mentioned, finite N-effects play a relevant role in the dynamics. Due to self-consistency, they are responsible for the fluctuations in time of the mean-field quantities $M_{1,2}$ and $P_{1,2}$. The potential experienced by each particle thus fluctuates in time and particles having an energy close to V_s have the possibility to be trapped in the potential as well as to escape from it. This implies that the localization phenomena illustrated in Fig.8 are not only due to bounces of the particle on the maxima of the potential, but also to trapping in the potential well itself due to separatrix crossing.

We have argued from simple considerations that diffusion should be anomalous in the collapsed phase. This is indeed the case, as confirmed from direct evaluations of the MSQD in a quite extended energy interval. An example of this is reported in Fig.9 for $U = 1.1$ and $N = 4,000$. Diffusion is anomalous for times smaller than a crossover time τ beyond which the Einstein's diffusion law is recovered $< r^2(t) >= 4Dt$. A similar behaviour for the

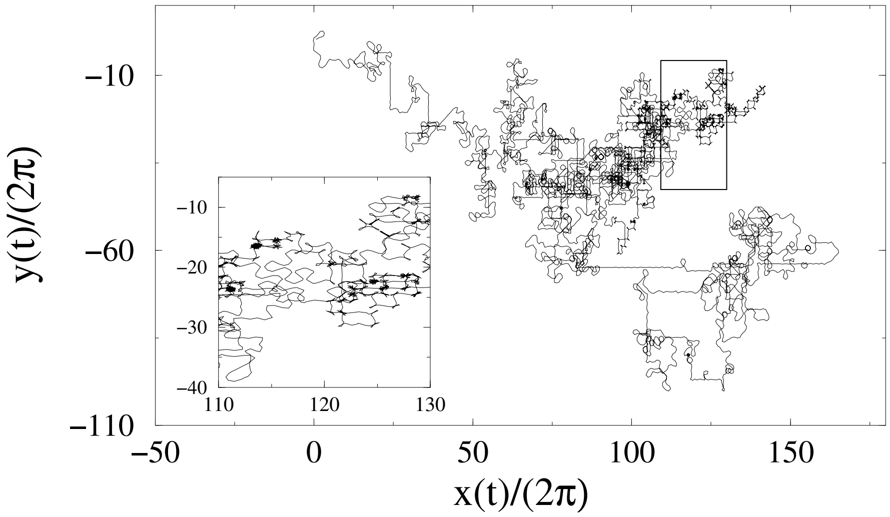

Figure 8. Typical time evolution of a particle initially in a channel of the 2D single particle potential 15. In this representation, the $2-D$ torus on which the dynamics takes place is unfolded and represented as an infinite plane constituted of an infinite number of juxtaposed elementary periodic cell of size 1×1. In the inset an enlargement of the trajectory in the indicated box is reported.

MSQD was previously observed for a system of N symplectic (globally and locally) coupled maps [33,34], but with a subdiffusive (i.e. with $\alpha < 1$) short time dynamics.

The energy dependence of the α-values is illustrated in Fig. 4. It shows up clearly that the thermodynamical phase transition from collapsed to homogeneous phase is associated to a dynamical transition from superdiffusion (with $1.3 < \alpha < 1.9$ for $0.4 \leq U < 2.0$) to ballistic motion (with $\alpha \simeq 2$ for $U \geq U_c$). In the collapsed regime, we observe an increase of α from 1.3 ± 0.1 to 1.9 ± 0.1, that is due to the modification of the shape of the single particle potential.

A possible explanation of this behaviour is the following. At very low energy $U < 0.3$, all the particles are essentially trapped in the potential well and none is channeling: no diffusion is observed in this case. For increasing energy a fraction of particles (due to the decrease of $V_M - V_m$) escapes from the well and some of them get enough energy to move along the channels: anomalous diffusion is then evidenced. The increase in the value of the exponent α is

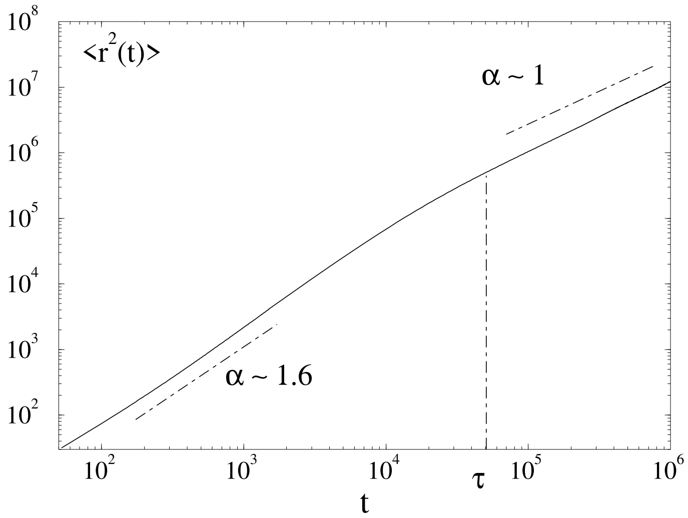

Figure 9. Time dependence of the mean square displacement $< r^2(t) >$ in a log-log scale for $U = 1.1$ and $N = 4,000$ for the 2D model. The solid line indicate the simulation results. The dot-dashed segments are the estimated slopes of $< r^2(t) >$ for $t < \tau$ and $t > \tau$.

due to the fact that also the channels width $V_M - V_s$ grows with U. However, for U approaching U_c the number of untrapped particles increases noticeably, but now the channel width vanishes abrubtly. This implies that a significant fraction of particles will move freely (with energy $> V_M$). These mechanisms lead naturally to ballistic motion for $U > U_c$, where the potential V_i is now almost constant apart from fluctuations of order $\mathcal{O}(1/\sqrt{N})$.

The fact that in the asymptotic limit ($t \to \infty$) normal diffusion is recovered constitutes a typical signature of a noisy dynamics [36,37,33]. But in our system no external noise is added to the system, therefore the transition from anomalous to asymptotic ordinary diffusion must be attributed to a "deterministic source of noise", that is intrinsic in our system and due to finite size effects.

A deterministic anomalously diffusing dynamical system submitted to weak environmental white noise shows a transition from anomalous diffusion to standard diffusion on sufficiently long time scales [36]. The crossover time τ for this transition can be explicitely computed [36] and turns out to increase as an inverse power law of the noise amplitude, when short time behaviour is superdiffusive.

When analyzing the N dependence of τ for two energies, $U = 1.48$ and $U = 2.0$, we find that $\tau \propto N$. The interpretation of the N dependence of the crossover time is straighforward if we consider finite N effects as a source of noise in our model, with a typical amplitude of order $1/\sqrt{N}$. This last assumption is justified by the fact that the microscopic dynamics of the particles generates stochastic fluctuations $O(1/\sqrt{N})$ in the values of M and P. These fluctuations become weaker for increasing N and thus naturally yield an increasing value of τ. More details about the relevant dynamical mechanisms can be found elsewhere [5].

We would like to stress that in the mean-field limit the diffusion will be anomalous at any time, while for finite N normal diffusion will be always recovered asymptotically. The fact that the dynamics of the system is strongly influenced by the order in which the two limits $N \to \infty$ and $t \to \infty$ are taken should be related to the long-range nature of the forces present in our model.

5 Chaotic properties

In order to complete the description of the two models, we investigate in this Section a fundamental indicator that characterizes the dynamics of Hamiltonian systems: the maximal Lyapunov exponent λ. Our analysis relies on numerical estimations of λ, performed considering the evolution in the tangent space and applying the standard technique first introduced in Ref. [38].

Our models are integrable in the limit of low and high energy, therefore $\lambda \to 0$ both for $U \to 0$ and $U \to \infty$. In between these two extrema we expect that a finite Lyapunov exponent will be observed.

5.1 One dimensional model

The 1D model is Lyapunov unstable ($\lambda > 0$) over all the energy range, see Fig. 10 (the maximal Lyapunov exponent of model (1) was first computed in Ref. [39]). Below $U \approx 0.2$ there is a weak size dependence of the Lyapunov exponent and a substantial independence on the chosen initial condition. A scaling law $\lambda \sim U^{1/2}$ is clearly visible (see Fig. 11a) and still lacks a convincing theoretical explanation (the theoretical expression derived in Ref. [40] gives $\lambda \sim U$, in sharp disagreement with numerical data); an argument, reported in Ref. [15] heuristically justifies the correct scaling. For $U > 0.2$, λ rapidly increases and reveals a strong dependence on N. In fact, it can be shown that in all the vanishing M phase ($U > U_c$), λ vanishes as $N^{-1/3}$ (see Fig. 11b)). This scaling is easily obtained resorting to a random matrix approximation of the dynamics [15], which considers the successive Jacobians as random and statistically independent, and has been also derived theoretically in Ref. [40] using differential geometric techniques. Moreover, also in true one dimensional gravitational models λ vanishes as an inverse power law of N as shown in [19,41] (in those cases the exponent ranges from $1/5$ to $1/4$). For true 3D gravitational models Gurzadyan and Savvidy, by relating the average Riemaniann curvature to the corresponding Lyapunov spectrum, were able to suggest the following scaling law [42] :

$$\lambda_G \propto \frac{GMN^{2/3}}{V^{2/3} < v >} \tag{21}$$

As already reported in Sec. 2.1, our models can be connected to true gravitational models by simply changing the time scale by a factor $1/\sqrt{N}$, since in our model the mass M is unitary, the gravitational constant G is dimensionless, and the volume $V = (2\pi)^d$ (where d is the dimension of the system) do not depend on N. Therefore it is sufficient in Eq.(21) to rescale the average velocity of the particles $< v >$ and the Lyapunov exponent by a factor $\sqrt{N}$. After such rescaling one obtains from Eq.(21) $\lambda \propto N^{-1/3}$. This suggests the validity of our results also in the 3D gravitational case. The maximal Lyapunov exponent relaxes to its asympotic value with a $N^{-1/3}$-law also for a gas of hard-spheres [43]: this universality would deserve further investigation.

Although the strong N dependence hides the effect, an evident peak of λ is present just below the phase transition point, in correspondence of the negative specific heat region. Chaos is "stronger" in this region due to the contribution of particles which evaporate from the cluster, entering the stochastic layer near the separatrix. The curious coexistence of negative specific heat, superdiffusion and maximal chaos deserves further studies. A confirmation of such a behavior of the maximal Lyapunov exponent for systems with long-range interactions can be found in Ref. [21], where, slightly modifying model (1), it has been shown that when the interaction becomes short-ranged λ no more vanishes in the $N \to \infty$ limit. These authors further argue that the exponent $-1/3$ of the infinite-range model modifies continuously by reducing the range of the interaction, reaching zero when the interaction becomes short-ranged.

5.2 Two dimensional model

Our data for the 2D model (9) are reported in Fig. 12 for three different types of initial conditions :

- (A) Maxwellian velocity distribution and clustered particles;

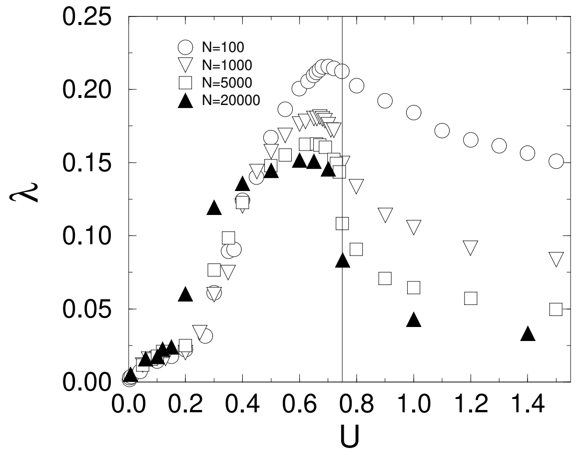

Figure 10. Maximal Lyapunov exponent λ as a function of the internal energy for the 1D model (1) for increasing N. The system has been started from equilibrated initial data.

- (B) Maxwellian velocity distribution, but with a thermal velocity coinciding with its canonical prediction, and particles spatially organized in a single cluster in such a way that also the M- and P-values reproduce the canonical prediction;

- (C) water-bag velocity distribution and clustered particles.

The initial condition (C) is the one commonly used through the present paper, in particular for the study of transport in the system. As it can be seen from Fig. 12 , λ grows for increasing U up to a maximum value and then decreases. Such maximum (at least for $N = 200$) is located at an energy $U \simeq 1.3 - 1.4 < U_c$. For $U > U_c$, we observe a power law decrease of λ with N with an exponent ~ 0.31 in good agreement with the results for the 1D model.

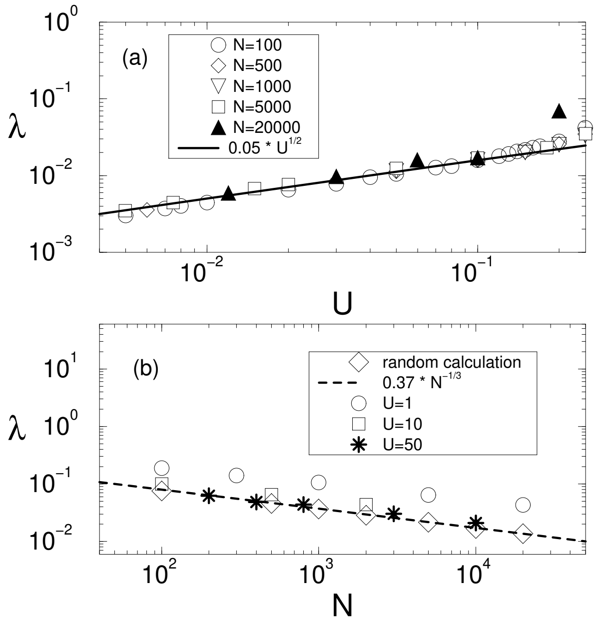

Figure 11. a) Maximal Lyapunov exponent λ vs. the internal energy U for the 1D model various systems sizes N, showing N-independence and the $U^{1/2}$ common scaling. b) λ vs. N for various values of $U > U_c = 0.75$. For increasing value sof U the scaling law $N^{-1/3}$ is verified better and better. The stars refer to a simulation performed with random Jacobians, showing the effectiveness of the random matrix approximation.

In our model the vanishing of λ in the mean-field limit, for $U > U_c$, is connected to the fact that the single particle potential becomes flat and the system integrable.

In the low energy limit (for $U < 0.01$) a power law increase of the type $U^{1/2}$ is clearly observable for all the three types of initial conditions similarly to 1D. This indicates that for fully coupled Hamiltonian systems this property holds in general, independently of the space dimensionality. In particular, for $U \to 0$ the particles are all clustered, therefore we expect that the scaling $\lambda \propto U^{1/2}$ should be related to a "collective" chaotic mechanism.

Let us now discuss the mechanisms behind the observed behaviours of λ. Once the energy U is fixed for all the three considered initial conditions, after a reasonable transient, we obtain exactly the same values for the aver-

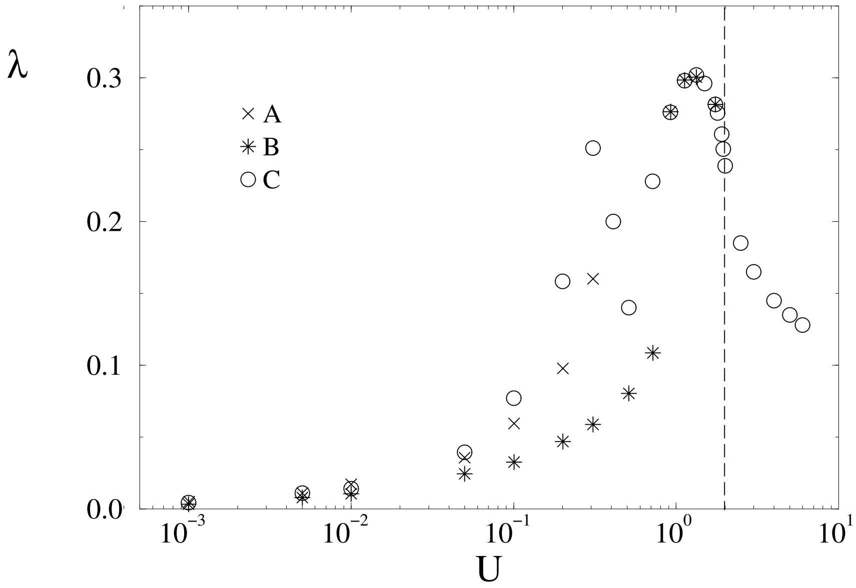

Figure 12. Maximal Lyapunov exponent as a function of U in a log-linear plot, for three different initializations of the 2D model. The dashed line indicates the critical energy U_c. The reported data corresponds to $N = 200$ and to integration times ranging from $t \sim 1 \times 10^6$ to $t \sim 9 \times 10^6$.

age temperature T and magnetizations M and P and a common Maxwellian distribution for the velocities. However, at low energies ($0.001 < U < 0.8$) the measured average λ depends heavily on the initial conditions. This clearly indicates the coexistence of several equivalent states, that can be considered as equilibrated within the examined time interval. Evidently the measurement of λ is more sensible to the presence of such equivalent states than that of thermodynamical variables. It should be noticed that this kind of behaviour is unexpected in N-body Hamiltonian systems, because it is commonly believed that for sufficiently large values of N Arnold diffusion takes place and each orbit is allowed to visit the full phase-space. But our data instead indicate that some "barrier" in the phase space still survive even for $N = 200$. The origin of this lack of ergodicity is related to the long range nature of the forces that induces a persistent memory of the initial conditions, as previously noticed by Prigogine and Severne [13] for gravitational plasmas. Recently, some numerical evidence of non ergodicity has been reported also for 1D gravity

[19,41]. But ina recent paper [44] this evidence is questioned in favour of a slow relaxation mechanism affecting high energy particles.

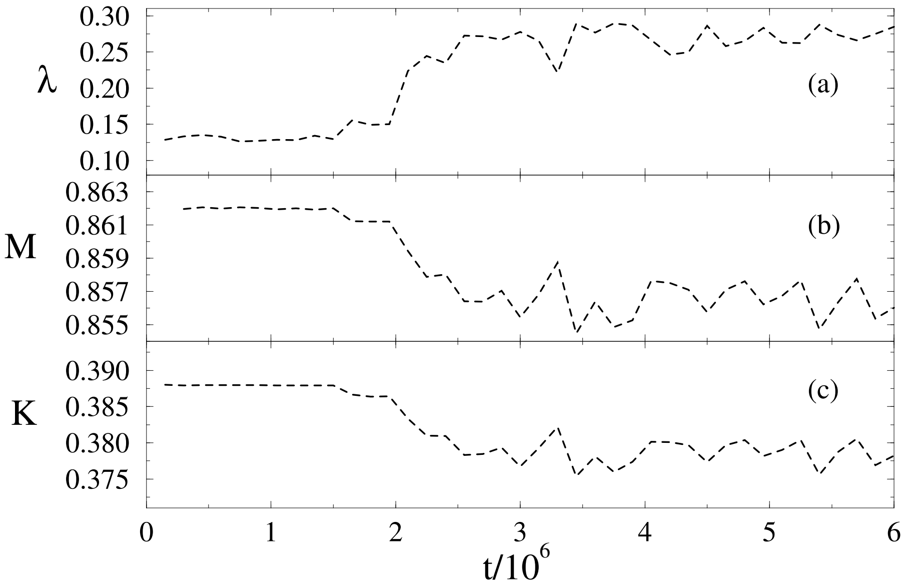

Figure 13. Time evolution of the maximal Lyapunov exponent λ, of the magnetization M, and of the kinetic energy K are shown for a initial condition of (B)-type for the 2D model at $U = 0.87$ and with $N = 200$.

It is clear from Fig.12 that, in the interval $U \in [0.001, 0.8]$, for initial conditions of type (B) λ remains always smaller than the corresponding exponents obtained with initial conditions (A) and (C). The maximal differences are observed in the energy range $0.2 < U < 0.8$, where particles begin to escape from the cluster (this happens for initial conditions (A) and (C)). Above $U \simeq 0.9$ the same Lyapunov is obtained for all types of initial conditions. A typical feature of initial conditions (B), for $U < 0.8$ is that all the particles are trapped in the potential well. Instead when one or more particle escape from the cluster ($U > 0.9$) also with this initial condition the common value of λ is obtained. Indeed, two chaotic mechanisms are present in the system: one felt by the particles moving in the minimum of the potential and one by particles visiting a region near to the separatrix. This second mechanism is well known and it is related to the chaotic layer around the separatrix. The former one is due to the erratic motion of the minimum of the potential well. In order to clearly identify such mechanisms we have followed the trajectory of a system initially prepared in condition (B) for an energy $U = 0.87$ and $N = 200$. On a short time scale all the particles are trapped and we measure an average value $\lambda \simeq 0.13$. When at a later time one particle escapes from the cluster λ almost doubles its initial value (see Fig. 13). In Fig. 13 the magnetization M and the kinetic energy K are also shown. When the particle escapes from the cluster M shows a clear decrease as well as K. This last effect is due to the fact that potential energy V is minimal when all the particles are trapped, therefore if a particle escapes V increases and, due to energy conservation, K decreases. This is the phenomenon underlying the negative specific heat effect. From the above arguments we can identify a "strong" chaos felt from the particles approaching the separatrix and a "weak" chaos associated to the orbits trapped in the minimum of the potential. The presence of these two chaotic mechanisms, together with the non-ergodicity of the system, explains the strong dependence of the values of λ on the initial conditions.

6 Conclusions

This paper reviews, discussing differences and similarities, a class of models of point masses without hard-cores and interacting with an infinite-range attractive potential in one and two dimensions. Both models may be seen as toy systems for studying long-range attractive interactions in an extremely simplified setting. We consider them a dynamical extension of the lattice gas model introduced and studied by Hertel and Thirring [9]. Thirring [8,9] pointed out that a transition from a clustered to a homogeneous phase can be associated with a negative specific heat (within the microcanonical ensemble) either (I) when the potentials are thermodynamically unstable [8] or (II) when the thermodynamical potentials are extensive quantities, but the interaction is long-ranged (at least in the limit $N \to \infty$). In a true gravitational potential both the above conditions are fulfilled. Studies of N-body models with short-range thermodynamically unstable potentials [29,30] confirmed that condition (I) was sufficient to observe transition from a clustered to a gaseous phase, negative specific heat, inequivalence of canonical and microcanonical ensemble. Our studies concerns a continuous time model with thermodynamically stable potential ($H_N \geq E_0 N$), but with long-range attractive interaction. Therefore they confirm that the characteristic associated to the transition observed by Hertel and Thirring for a simple lattice gas model are present also in more realistic models and that condition (II) is indeed a sufficient one. Let us try to summarize condition (I) and (II) in an unique prescription : *in order to observe a transition belonging to the Hertel and Thirring universality class it* *is necessary that the thermodynamical potentials (e.g. the entropy) are not additive even in the limit $N \to \infty$ and that the interaction is attractive* [45]. In other words if a system composed by an infinite number of particles is splitted in two sub-systems typically any thermodynamical potential of the whole system coincide with the sum of the entropies of the two sub-systems, if this is not the case violation of the standard thermodynamics should be expected.

Moreover, we show here that extremely simple infinite-range mean-field models display several interesting features, which are present also in gravity in one and two dimensions (we believe that our approach can be extended to three dimensions without conceptual difficulties). A drawback of our models is that the microcanonical solution has not yet been obtained exactly and we must rely on numerical simulations (apart from some results which can be obtained by the collisionless Boltzmann-Poisson equation). This drawback turns however into an advantage if one is interested in dynamical effects, about which thermodynamics gives no hint. The main dynamical effect discussed in this review is "superdiffusion" (the particles mean square displacement grows faster than linear with time). Superdiffusion is present in the region of negative specific heat and is due to the particles which evaporate from the cluster and perform long flights before being trapped again (the configuration space is a torus). Evaporation is also the source of "strong" chaos: in the negative specific heat region the maximal Lyapunov exponent λ is much larger than everywhere else. Although gravity has no phase transition in 1D (the gravitational system is always clustered) and the question is open whether a phase transition is present in 2D [7], both the effects discussed above could be present in the negative specific heat region of self-gravitating systems, and we do not see any obstruction to their existence also in 3D. Finally, let us comment on a few scaling laws that we have found to be universal for all the models of the class we have introduced. In the gaseous phase the maximal Lyapunov exponent λ vanishes as $N^{-1/3}$ in analogy with what is found for some specific gravitational systems and for other dynamical models of fluids [42,43]. In the low energy clustered phase $\lambda \sim U^{1/2}$. This should be true also in 3D and could be checked in "true" self-gravitating systems in their collapsed low-energy phase.

Acknowledgments

This review is an account of an ongoing joint collaboration of the authors with V. Latora and A. Rapisarda; many of the results here reported stem from discussions with them and are part of common papers. We also thank Andrea Rapisarda for furnishing updated versions of some figures. We acknowledge useful discussions with D. Mukamel, W. Hoover, H.A. Posch, and H. Spohn. We also are grateful to the DOCS research group (see *http://docs.de.unifi.it/∼docs*) in Firenze for stimulating interactions. M.A. thanks Dr. J. Kister for his determinant help during his installation in Marseille and J. Albertini for fruitfull computational help.

References

1. L. Landau and E.M. Lifsits, *Fisica Statistica* (Editori Riuniti, Roma, 1978).
2. C. Tsallis, *Braz. J. of Phys.*, **29**, 1 (1999) (cond-mat/9903356).
3. D. Lynden-Bell, Proceedings of the XXth IUPAP International Conference on Statistical Physics, Paris, July 20-24 (1998); for a recent review see also cond-mat/9812172.
4. S. Ruffo, in *Transport and Plasma Physics*, edited by S. Benkadda, Y. Elskens and F. Doveil (World Scientific, Singapore, 1994), pp. 114-119; M. Antoni and S. Ruffo, *Phys. Rev.* E **52**, 2361 (1995).
5. M. Antoni and A. Torcini, *Phys. Rev.* E **57**, R6233 (1998); A. Torcini and M. Antoni, *Phys. Rev.* E **59**, 2746 (1999).
6. P.H. Chavanis, J. Sommeria and R. Robert, *Astroph. Journal*, **471**, 385 (1996); P.H. Chavanis and J. Sommeria *Mon. Not. R. Astron. Soc.*, **296**, 569 (1998).
7. E. Abdalla and M. Reza Rahimi Tabar, hep-th/9803161.
8. W. Thirring, *Z. Phys.*, **235**, 339 (1970).
9. P. Hertel and W. Thirring, *Ann. of Physics*, **63**, 520 (1971).
10. M. Antoni, H. Hinrichsen and S. Ruffo, cond-mat/9810048.
11. S. Inagaki, *Progr. Theor. Phys.*, **90**, 577 (1993); S. Ingagaki and T. Konishi, *Publ. Atron. Soc. Jpn.*, **45**, 733 (1993).
12. S. Ruffo, unpublished results.
13. I. Prigogine and G. Severne, *Physica* **32**, 1376 (1966).
14. K. Kaneko and T. Konishi, *J. Phys. A: Math. Gen* **25**, 6283 (1992); *Physica D* **71**, 146 (1994).
15. V. Latora, A. Rapisarda and S. Ruffo, *Phys. Rev. Lett.* **80**, 692 (1998); *Physica* D **131**, 38 (1999).
16. J. L. Rouet and M. R. Feix, *Phys. Rev.* E **59**, 73 (1999).
17. M. Antoni, Y. Elskens and C. Sandoz, *Phys. Rev.* E **57**, 5347 (1998).
18. Y. Elskens and M. Antoni, *Phys. Rev.* E **55**, 6575 (1997).
19. L. Milanović, H. A. Posch and W. Thirring, *Phys. Rev.* E **57**, 2763 (1998).
20. J. H. Oort, *Bull. Astron. Inst. Netherlands* **6**, 289 (1932), G. L. Camm,

Mon. Not. R. Astron. Soc. **110**, 305 (1950).
21. C. Anteneodo and C. Tsallis, *Phys. Rev. Lett.* **80**, 5313 (1998).
22. M. K. H. Kiessling, *J. Stat. Phys.* **55**, 203 (1989).
23. B.N. Miller and P. Youngkins, *Phys. Rev. Lett.* **81**, 4794 (1998).
24. E.A. Novikov, *Sov. Phys. JETP* **41**, 937 (1975); H. Aref, *Ann. Rev. Fluid Mech.* **15**, 345 (1983).
25. D. Lynden-Bell and R. Wood, *Mon. Not. R. Astr. Soc.* **138**, 495 (1968); D. Lynden-Bell and R. M. Lynden-Bell, *Mon. Not. R. Astr. Soc.* **181**, 405 (1977).
26. J. Perez, private communication.
27. L. Casetti, E.G.D. Cohen, and M. Pettini *Phys. Rev. Lett.* **82**, 4160 (1999).
28. T. Geisel, in *Lévy Flights and related topics in physics*, Eds. M. F. Schlesinger *et al.* (Springer Verlag, Berlin, 1995) p 153 (see references therein); J. Klafter and G. Zumofen, *Phys. Rev.* E **49**, 4873 (1994); D. K. Chaĭkovsky and G. M. Zaslavsky, *Chaos* **1** (4), 463 (1991).
29. A. Compagner, C. Bruin, and A. Roesle, *Phys. Rev.* A **39**, 5989 (1998).
30. H.A. Posch, H. Narnhofer and W. Thirring, *Phys. Rev.* A **42**, 1880 (1990); *Physica* A **194**, 482 (1993).
31. V. Latora, A. Rapisarda and S. Ruffo, to be published in *Phys. Rev. Lett.* in 1999 (cond-mat/9904389).
32. J. Klafter, G. Zumofen and M. F. Schlesinger in *Chaos: the interplay between stochastic and deterministic behaviour* , eds. P. Garbaczewski et al. (Lecture Notes in Physics, Springer , Berlin, 1995) **457** p. 183 (see also references herein).
33. T. Konishi, Prog. Theor. Phys. **98**, 19 (1989); K. Kaneko and T. Konishi, *Phys. Rev.* A **40**, R6130 (1989).
34. T.Konishi and K. Kaneko, J. Phys. A: Math. Gen **23**, L715 (1990).
35. P. Grigolini, in *Chaos: the interplay between stochastic and deterministic behaviour* , eds. P. Garbaczewski et al. (Lecture Notes in Physics, Springer , Berlin, 1995) **457** p. 101.
36. E. Floriani, R. Mannella, and P. Grigolini, *Phys. Rev.* E **52**, 5910 (1995).
37. R. Bettin, R. Mannella, B.J. West and P. Grigolini, *Phys. Rev.* E **51**, 212 (1995).
38. I. Shimada and T. Nagashima, Prog. Theor. Phys. **61**, 1605 (1979); G. Benettin, L. Galgani, A. Giorgilli and J.M. Strelcyn, Meccanica, March 15 and 21 (1980).
39. Y.Y. Yamaguchi, Progr. Theor. Phys., **95**, 717 (1996); Int. J. Bif. Chaos, **7**, 839 (1997).
40. M.-C. Firpo, *Phys. Rev.* E **57**, 6599 (1998).

41. T. Tsuchiya, T. Konishi and N. Gouda, *Phys. Rev.* E **50**, 2607 (1994).
42. V.G. Gurzadyan and G.K. Savvidy, *Astron. Astrophys.*, **160**, 203 (1986)
43. Ch. Dellago and H.A. Posch, *Physica A*, **240** 68 (1997).
44. J. Makino, preprint (astro-ph/99032380).
45. D. Mukamel, private communication.